The Astrophysical Journal Letters, 761:L1 (4pp), 2012 ??? doi:10.1088/2041-8205/761/1/L1

REVERSE RADIATIVE SHOCK LASER EXPERIMENTS RELEVANT TO ACCRETING STREAM–DISK IMPACT IN INTERACTING BINARIES

C. M. Krauland[1], R. P. Drake[1], C. C. Kuranz[1], B. Loupias[2], T. Plewa[3], C. M. Huntington[1], D. N. Kaczala[1], S. Klein[1], R. Sweeney[1], R. P. Young[1], E. Falize[2], B. Villette[2], and P. A. Keiter[1]
[1] Department of Atmospheric, Oceanic, and Space Sciences, University of Michigan, Ann Arbor, MI 48109, USA; krauland@umich.edu, rpdrake@umich.edu
[2] CEA-DAM-DIF, F-91297 Arpajon, France
[3] Department of Scientific Computing, Florida State University, Tallahassee, FL 32306, USA
Received 2012 February 24; accepted 2012 November 7; published 2012 ???

ABSTRACT

We present the first results from high-energy-density laboratory astrophysics experiments that explore the hydrodynamic and radiative properties of a reverse shock relevant to a cataclysmic variable system. A reverse shock is a shock wave that develops when a freely flowing, supersonic plasma is impeded. In our experiments, performed on the Omega Laser Facility, a laser pulse is used to accelerate plasma ejecta into vacuum. This flow is directed into an Al plate in front of which a shock forms in the rebounding plasma. The plasma flow is moving fast enough that it is shocked to high enough temperatures that radiative cooling affects the shock structure. These are the first experiments to produce a radiative reverse shock wave.

Key words: accretion, accretion disks – methods: laboratory – novae, cataclysmic variables – shock waves

Online-only material: color figures

1. INTRODUCTION

Over the last half century, there has been extensive astrophysical research on dwarf novae, novae, and nova-like systems, which are categorized as cataclysmic variables (CVs) (Warner 1995). Most often CVs are binary star systems in which one star is a white dwarf (WD) and the other star is a late-type main-sequence star. Much of this work has shown that the nature of CVs depends on the gas flow from the cool star (i.e., the secondary) to its WD companion (Livio 1993). As mass flows away from the secondary star, it fills the system's largest closed equipotential surface, the Roche lobe, and overflows (Crawford & Kraft 1956; Paczynski 1971). This mass is lost through the inner Lagrangian point (L1) and falls toward the WD in a supersonic stream maintaining its initial coherence (Lubow & Shu 1975). The CVs of interest here feature an accretion disk. Early in the secondary's mass donation, conservation of angular momentum and viscous processes cause the stream to flow around the WD (with the trajectory lying entirely in the orbital plane of the binary) and spread into an accretion disk (Verbunt 1982). The gas stream that leaves L1 in approximate vertical hydrostatic equilibrium continues to flow along the same ballistic trajectory even after the disk is established (Lubow & Shu 1976). As it does so, it now strikes the outer regions of the disk with highly supersonic velocity. This produces a localized shock-heated area that may radiate as much or more energy at optical wavelengths as the WD, secondary, and disk combined (Warner 1995). The resulting emission feature is commonly referred to as the *hot spot* or *bright spot*.

Observations in the emission line spectrum of CVs indicate that *hot spot* existence stems from the disk–stream interaction. Recorded spectra show very strong, double H emission lines that are stationary and believed to be produced in the disk. On top of these, however, there is a weak H emission line that varies in radial velocity and forms an "S-wave" between the stationary lines (Kraft 1961; Krzeminski & Kraft 1964). The fact that the S-wave component is fairly sharp compared to the total width of the emission lines indicates that it originates in a relatively small region of higher temperature (Livio 1993). Furthermore, particular CV data of S-wave amplitude and phase suggest that the velocity vector of the emitting atoms is either nearly identical to the incoming gas stream near the point of collision or that it shares the rotational velocity of the disk and the emitting atoms are located on the outer parts of the disk (Krzeminski & Smak 1971). These two scenarios differ in how and where the stream material interacts with disk, suggesting that the S-wave emission can originate in either (1) stream flow above and below the disk or (2) a collided flow bulge at the outer disk edge (Smak 1985). Much eclipse data support the occurrence of both of these situations (Thorstensen et al. 1991; Hellier 2000; Smak 2003; Spruit 2005).

The radiative cooling properties of the strongly radiating shock that forms in the accreting stream may determine which of these scenarios is dominant. Simulations conducted prior to the present experimental work suggest that altering the cooling efficiency of the hot spot region can produce both scenarios of dynamic evolution (Rozyczka & Schwarzenberg-Czerny 1987; Armitage & Livio 1998). In terms of radiative shock systems, the cooling efficiency of the system is determined by the optical depth of the shocked material. Efficient cooling occurs in optically thinner systems, while optically thick systems better confine radiation.

The ability of high-intensity lasers to create large energy densities in targets of millimeter-scale volume makes it feasible to create radiative shocks in the laboratory (Bouquet et al. 2004; Reighard et al. 2006; Doss et al. 2010). They also grant us the ability to define the optical depth profile given chosen materials. However, a new approach is necessary in order to observe dynamics relevant to CVs. This work is the first report of an experimental system that can explore the creation of a radiative shock in freely flowing supersonic plasma streams in the laboratory. Here we report the production of collimated, accelerating plasma ejecta that collide with a static wall and form a radiative reverse shock in the rebounding flow.

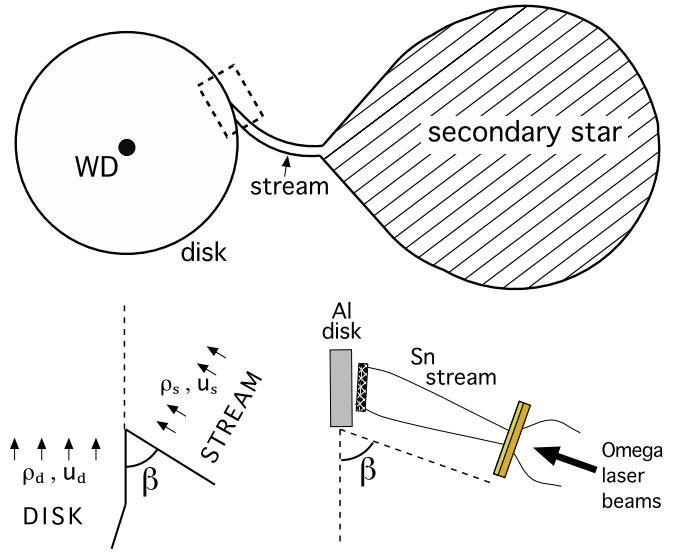

Figure 1. Top: general schematic of CV orbital plane, with dashed rectangle highlighting the "hot spot" area of interest. Bottom left: basic geometry of stream–disk impact. Bottom right: designed geometry of the laboratory experiment.

(A color version of this figure is available in the online journal.)

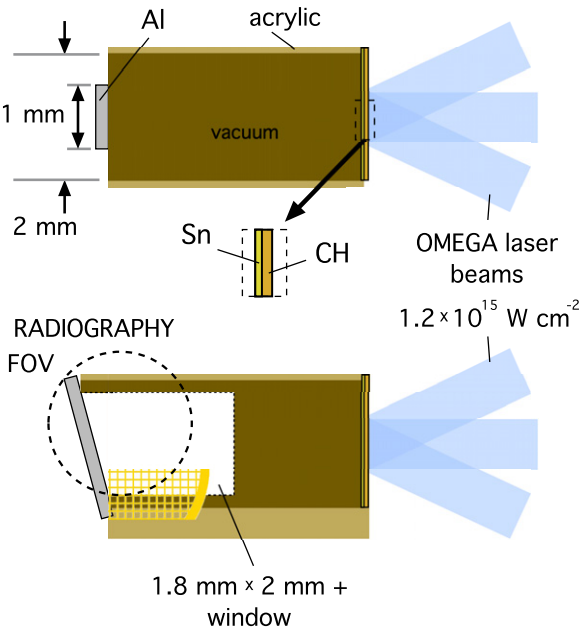

Figure 2. Two orthogonal views of the target design. Bottom: radiography view. The main laser pulse comes from the right. After the laser pulse turns off, Sn ejecta expand to the left, down the evacuated target tube toward the 100 μm Al wall roughly 4 mm away. A window is extracted from the acrylic target superstructure so that we do not image through any walls in the radiograph. Top: optical pyrometer view. The Al end wall does not cover the entire diameter of the tube in this direction, so Sn plasma can stream out of the tube, unshocked, around the wall. Note: not to scale.

(A color version of this figure is available in the online journal.)

The configuration also provides the opportunity to observe the emission "light curve" from the shock front. This approach sets up future experiments that will replace the static wall with a secondary flowing plasma, more analogous to the *hot spot* system from the accretion stream–disk impact.

2. EXPERIMENTAL SETUP

Our experiments were performed on the Omega Laser Facility (Soures et al. 1996) at the Laboratory for Laser Energetics, using the target configuration shown in Figure 2. In order to create a supersonic directed plasma flow, we ablate the plastic coated side of an Sn foil in vacuum. The foil, 10 μm of CH deposited on 5 μm of Sn, is attached to one side of an evacuated 2 mm diameter cylinder. The tube is milled out of an acrylic box such that the face on which the CH/Sn foil is glued is normal to the tube axis. The other end of the target cylinder is machined $\sim$15° off of the axis normal, such that an Al foil can be attached at an oblique angle. The 2.0 mm by 1.0 mm strip of 100 μm thick Al foil is centered around the tube axis such that it extends over the diameter in only one side view, shown in Figure 2.

The experiments on OMEGA-60 employ a laser configuration of 10 beams with $\sim$4.5 kJ of energy, 1 ns pulse, and 704 μm diameter spot produced by distributed phase plates. Because the CH/Sn foils are thin, beam smoothing by spectral dispersion is also used. With an irradiance of $\sim 10^{15}$ W cm^{-2}, the laser ablation pressure ($\sim$40 Mbar) will shock and accelerate the Sn. After the laser pulse, the Sn plasma will expand, cool, and accelerate down the target cylinder. Eventually the Sn plasma will reach the dense end wall of Al. In response, a reverse shock will develop in the flow and a forward shock will be driven into the end wall. The geometry lends itself to good diagnostic access for the shocked layer.

2.1. Timescales and Similarity Properties

In the CV system, there is an enduring supersonic gas flow from the secondary star toward the WD, which may or may not be steady. The "enduring" part of that system is a challenge for laser-driven experiments, in which the amount of mass involved in the fluid flow is limited by the deposited laser energy on the target. This amount of mass dictates how long we can produce a quasi-steady flow of plasma. In turn, this dictates the timescale of the experimental conditions. We approximate the forward motion of the Sn plasma as homologous expansion, signifying that the fractional rate of change of velocity is constant at least up until the terminal velocity. In other words, $v \propto d/t$. Considering a terminal velocity, $v_{\rm max} \sim 200$ km s^{-1} based on simulation, and a radiative threshold velocity (Drake 2004) of $v_{\rm rad} \sim 100$ km s^{-1}, we can estimate the radiative phase to be 20 ns based on our $\sim$4 mm long target. This timescale suggests a large enough experimental window to diagnose a radiative shock in our target geometry.

Another distinction should be made in comparing our experimental system to that of the CV. Arguments made by Armitage & Livio (1998) suggest that the optical depth profile of the shock system can change in the astrophysical system due the accretion rate itself. Because our experimental system is limited by laser energy and materials, we make some determination about what CV system this work can be applied to. Over the timescale of experimental significance, we can compare the main dimensionless numbers that characterize the laboratory and astrophysical shock systems (Ryutov 1999). In the hot spot case, the main parameters are the Mach number of the flow, the ratio of accretion disk to stream density, and the ratio of disk to stream scale heights. In addition, one can calculate two useful dimensionless numbers relevant to radiative shock systems. The first, designated $R_{\rm rad}$, is the ratio of material energy flux going into the shock front to the energy flux lost to radiation in an optically thick system at the immediate post-shock temperature.

Table 1
Main Dimensionless Numbers Characterizing the Hot Spot Regions and the Laboratory Plasma

Plasma Parameters	Hot Spot Regime	Laboratory Plasma
$T_{\rm ps}$ (eV)	100	200
$\rho_{\rm s}$ (g cm^{-3})	5×10^{-11}	10^{-2}
$u_{\rm s}$ (km s^{-1})	300	150
$\eta_o = \rho_{\rm s}/\rho_{\rm d}$	10^{-2}	10^{-2}
$h_{\rm s}/h_{\rm d}$	2	2
$M_{\rm s}$	30	10
$R_{\rm rad}$	6.5×10^{-7}	8.5×10^{-3}
χ	0.1	0.8

Notes. The indices s, d, and ps correspond to stream, disk, and post-shocked plasma.

Similar to the Boltzmann number (Mihalas & Weibel-Mihalas 1999), this ratio offers a measure of the relative importance between radiative and material energy transport in the radiating system. Because the increase of material enthalpy flux is balanced directly by the decrease in kinetic energy flux across the discontinuity, we represent $R_{\rm rad}$ here as

$$R_{\rm rad} = \frac{\frac{1}{2}\rho_o u_s^3}{\sigma T_{\rm ps}^4}, \quad (1)$$

where ρ_o and u_s are the density and velocity of the incoming flow, respectively, and $T_{\rm ps}$ is the post-shock temperature. If $R_{\rm rad}$ falls below 1, i.e., the continuum emission exceeds the material energy flux, the optically thick system would be violating energy balance, and so the structure of the shocked layer must change to prevent this. Therefore, when radiative energy transport is important one will have $R_{\rm rad} \ll 1$. The second parameter, known as the cooling parameter χ, provides a measure of the qualitative hydrodynamics of the flow. In the most general form, it is the ratio of cooling time to the dynamical time. Here we distinguish the determination of the ratio for both the laboratory and the CV. Following Blondin et al. (1995), a simple description of the cooling time at the hot spot is given by

$$t_{\rm cooling} \approx \frac{k_{\rm B} T_{\rm ps}^3}{n\Lambda(T_{\rm ps})}, \quad (2)$$

where $k_{\rm B}$ in the Boltzmann constant, n is the number density of electrons, and Λ is the cooling function which is taken from Dalgarno & McCray (1972) for this approximation. The dynamical time at the edge of the disk is simply $t_{\rm dynamic} \sim \Omega^{-1}$, where Ω is the Keplerian angular velocity and approximated to have a minimum on the order of 10^3 s. For the laboratory system, we follow Falize et al. (2011) and define the cooling time as

$$t_{\rm cooling} = \frac{p_{\rm shock}}{(\gamma - 1)\Lambda}, \text{ with } \Lambda \approx \sigma T_{\rm ps}^4 \kappa_{\rm p}, \quad (3)$$

where $\kappa_{\rm p}$ is the Planck mean opacity in Sn. The experiment dynamical time is the ratio of the shock height to u_s. Table 1 shows the values of the main physical quantities and these dimensionless numbers for both the astrophysical and laboratory plasmas. In the CV case, we use the regime of CVs and numbers given by Armitage & Livio (1998), while experimental values are taken from both simulation and laboratory data. Experimental design made a priority to conserve both the density ratio between the supersonic stream and the "disk," as well as the ratio of scale heights. With this and Mach numbers $\gg 1$, we should be producing similar impact physics with strong shocks. While B_o suggests both shocks are strongly radiating, it is having a comparable (invariant) χ between the laboratory and the CV system that suggests we can conceivably maintain the same balance between the radiation and hydrodynamic effects in the systems.

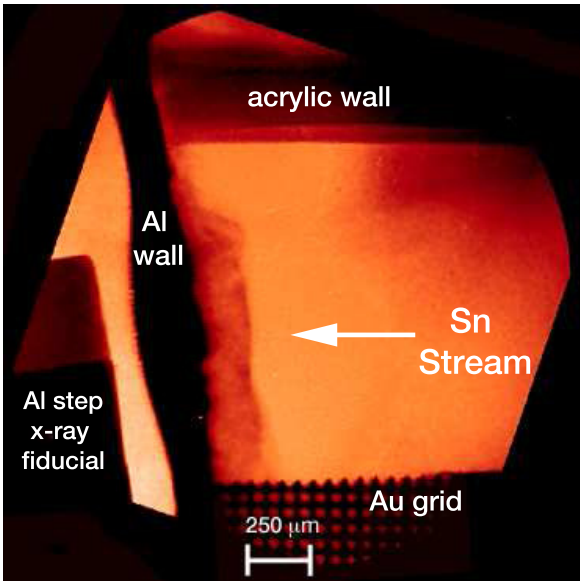

Figure 3. X-ray radiograph taken at 34 ns. Al end wall is ∼15° off of Sn flow normal. Au grid serves as a spatial and magnification fiducial.
(A color version of this figure is available in the online journal.)

3. EXPERIMENTAL RESULTS

We diagnose the density distribution within the reverse shock, and in the surrounding medium, by point projection X-ray radiography (Workman et al. 2004) using a laser-heated zinc plasma as the backlighting source. The He-α transitions in the Zn plasma illuminate a section of the target package through a 20 μm diameter pinhole, allowing a well-resolved image of the shock and target body to be captured on X-ray film. This radiograph is captured once per experimental shot. The exposure of the film is determined by ∼1 ns pulse length and the timing of secondary laser beams that irradiate the Zn foil. These secondary beams can be triggered at different times relative to the laser pulse on the main experimental target. An experimental radiograph is shown in Figure 3. It was captured 34 ns after the initial laser pulse on the CH/Sn foil and roughly 8 ns after the Sn first reaches the Al wall. This relative timing is confirmed using an X-ray diode spectrometer, called μDMX (Bourgade et al. 2001), that is positioned to obliquely observe the shock ∼30° from its normal. The spectrometer has numerous soft X-ray channels used to extract a time-resolved light curve from the strongly radiating phase of the shock.

In Figure 3, the thin dense shock can be seen just left of center. As the Sn flow comes from the right, it becomes shocked roughly 150 μm from the original Al wall position. To the left of the Al wall outside of the target structure and experimental influence, there are three varying thicknesses of Al foil. We use the attenuation profiles through these for X-ray background calibration and initial signal intensity from the backlighter. This information provides the ability to extract mass density profiles

from the radiograph, which suggests that we are seeing a thin compressed Sn layer. If Al was expanding from the wall and then being compressed by the plasma stream, this would produce a much denser layer than what was imaged.

A streaked optical pyrometer (Miller et al. 2007) is also employed at the orthogonal view to radiography on each shot, to corroborate timing with the self-emission in optical wavelengths. Because the emission is time-resolved and spatially resolved in one dimension, this also provides an average velocity for the stream and reverse shock.

We note that most data have shown that the lateral width of the observed shock is limited by target wall blowoff. As future experiments aim to diagnose the diverted flow in that direction as well, this interferes. A revision of target design will be made to greatly reduce the amount of wall near the end plate as we go forward.

4. CONCLUSIONS

The data on this novel high-energy-density experimental platform show a promising new approach to radiative shock waves. These radiative reverse shocks have upstream material velocity in the laboratory frame and are nearly steady over the timescale of diagnostic significance. Targets have been fielded to drive Sn plasma flows. We have taken X-ray radiographs of the reverse shocks created over a range of 10 ns. Ongoing computational work with the radiation hydrodynamics code CRASH (van der Holst et al. 2011) is being done in conjunction with this experimental work.

In connection with the CV system, the properties of the shock formed in the accreting plasma stream should dictate the way material moves around it. Scaling of relevant dimensionless parameters gives us a framework within which we can draw direct comparisons to the *hot spot* in the further development of these experiments. Our aim is to replace the Al end wall with a second, denser plasma flow as a surrogate for the accretion disk material, in conjunction with adjusting the relative scale heights of each flow. Understanding the accretion stream's dynamics at the *hot spot* and its integration into the disk can inform astrophysical theory and interpretation.

We are grateful to Chuck Sorce, Bruno Villette, and all assisting staff at LLE and CEA for diagnostic support.

This work is funded by the NNSA-DS and SC-OFES Joint Program in High-Energy-Density Laboratory Plasmas, by the National Laser User Facility Program in NNSA-DS, and by the Predictive Sciences Academic Alliances Program in NNSA-ASC. The corresponding grant numbers are DE-FG52-09NA29548, DE-FG52-09NA29034, and DE-FC52-08NA28616.

Facility: LLE

REFERENCES

Armitage, P. J., & Livio, M. 1998, ApJ, 493, 898
Blondin, J. M., Richards, M. T., & Malinowski, M. L. 1995, ApJ, 445, 939
Bouquet, S., Stehle, C., Koenig, M., et al. 2004, Phys. Rev. Lett., 92, 22
Bourgade, J. L., Villette, B., Bocher, J. L., et al. 2001, Rev. Sci. Instrum., 72, 1173
Crawford, J. A., & Kraft, R. P. 1956, ApJ, 123, 44
Dalgarno, A., & McCray, R. A. 1972, ARA&A, 10, 375
Doss, F. W., Drake, R. P., & Kuranz, C. C. 2010, High Energy Density Phys., 6, 157
Drake, R. P. 2004, Ap&SS
Falize, E., Michaut, C., & Bouquet, S. 2011, ApJ, 730, 96
Hellier, C. 2000, New Astron. Rev., 44, 131
Kraft, R. P. 1961, Science, 134, 1433
Krzeminski, W., & Kraft, R. P. 1964, ApJ, 140, 921
Krzeminski, W., & Smak, J. 1971, Acta Astron., 21, 133
Livio, M. 1993, in Accretion Disks in Compact Stellar Systems, ed. J. C. Wheeler (Singapore: World Scientific), 243
Lubow, S. H., & Shu, F. H. 1975, ApJ, 198, 383
Lubow, S. H., & Shu, F. H. 1976, ApJ, 207, L53
Mihalas, D., & Weibel-Mihalas, B. 1999, Foundations of Radiation Hydrodynamics (Mineola, NY: Dover), 410
Miller, J. E., Boehly, T. R., Melchior, A., et al. 2007, Rev. Sci. Instrum., 78, 034903
Paczynski, B. 1971, ARA&A, 9, 183
Reighard, A. B., Drake, R. P., Dannenberg, K. K., et al. 2006, Phys. Plasma, 13, 082901
Rozyczka, M., & Schwarzenberg-Czerny, A. 1987, Acta Astron., 37, 141
Ryutov, D., Drake, R. P., Kane, J., et al. 1999, ApJ, 518, 821
Smak, J. 1985, Acta Astron., 35, 351
Smak, J. 2003, Acta Astron., 53, 167
Soures, J. M., McCrory, R. L., Verdon, C. P., et al. 1996, Phys. Plasmas, 3, 2108
Spruit, H. C. 2005,
Thorstensen, J. R., Ringwald, F. A., Wade, R. A., et al. 1991, AJ, 102, 272
van der Holst, B., Toth, G., Sokolov, I. V., et al. 2011, ApJS, 194, 23
Verbunt, F. 1982, Space Sci. Rev., 32, 379
Warner, B. 1995, Cataclysmic Variable Stars (Cambridge: Cambridge Univ. Press)
Workman, J., Fincke, J. R., Keiter, P., et al. 2004, Rev. Sci. Instrum., 75, 3915